www.amlett.com, www.vbripress.com/aml, DOI: 10.5185/amlett.2016.6143 Published online by the VBRI Press in 2016

Study of laser beam modulation influence on structure of materials produced by additive manufacturing

Anna Okunkova[1*], Marina Volosova[2], Pavel Peretyagin[3], Ivan Zhirnov[1], Pavel Podrabinnik[1], Sergey V. Fedorov[2] and Andrey Gusarov[1]

[1]*Laboratory of innovative additive technologies, Moscow State University of Technology STANKIN, Vadkovskiy per. 1, Moscow, 127994 GSP-4, Russia*
[2]*Department of High-efficiency machining technologies, Moscow State University of Technology STANKIN, Vadkovskiy per. 1, Moscow, 127994 GSP-4, Russia*
[3]*Laboratory of electric current and sintering technologies, Moscow State University of Technology STANKIN, Vadkovskiy per. 1, Moscow, 127994 GSP-4, Russia*

[*]Corresponding author. Tel: (+7) 9099131207; E-mail: a.okunkova@stankin.ru

Received: 06 September 2015, Revised: 30 November 2015 and Accepted: 22 December 2015

ABSTRACT

In the article, the study of laser beam modulation influence on the structure of materials produced by one of the methods of additive manufacturing as selective laser melting (SLM) is provided. For the purpose of creating a smoother temperature gradient and the optimal conditions of the heat and mass transfer in the melting pool, an experimental stand for SLM-processing with the system of laser beam power density distribution modulation was created. The laser beam modulation gives promising results for higher parameters' combinations such as power more than 150W and scanning velocity more than 50 mm/sec. The single track's formation was produced by different power density distribution as Gaussian, Flat-top and Inverse Gaussian (Donut). All the received single tracks were studied with the use of optical and SEM microscopy. The results produce important data about reducing the width of powder consolidation zone, more even structure and higher productivity.

Keywords: Additive manufacturing; selective laser melting; laser beam modulation; structure of materials; video monitoring.

Introduction

Nowadays the methods of rapid prototyping and additive manufacturing grow very rapidly. One of the most advanced methods of solid growing is selective laser melting. The SLM is important in such industries as machine and aviation building and individual medical applications and sensors' industry [**1**]. The main principle of the method is layer-by-layer growing solids by remelting powders with laser beam in accordance with 3D models [**2**]. There are some problems yet to be solved in the productivity of the method. With increased laser source power, the productivity problem could not be resolved directly [**3**].

During the processing, the optical diagnostics of the process showed that there are the consciences of the thermal hit in the melting pool as powder granules' escape, interruption of the powder layer equability, Marangoni effect, active chemical interaction with camera environment, overheat and dynamic effects in the melting pool [**4**]. The problems concerned could be connected with the features of temperature gradients in the melting pool [**5**], which are the result of the power density distribution (TEM00).

In this paper, the development of optical assets for laser beam modulation for the purpose of improving the productivity of selective laser melting by the example of single track formation from CoCrMo powder was provided. The parameters of the system for experimental assets for alternative Gaussian laser power distribution were obtained. The approbation of the system was made using the methods of optical monitoring and diagnostics.

Table 1. Chemical composition of CoCrM powder.

Element	Co	Cr	Mo	Si	Mn	Fe	C	Ni
Content, %	60-65	26-30	5-7	>1	>1	>0,75	>0,16	>0,1

Experimental

As a material for the current research work, the commercially available powder of cobalt-chrome alloy CoCrMo was used (**Table 1**). This powder was produced by means of gas atomization and has spherical particle morphology, which is more preferable for SLM uses. The powder provides a spherical morphology that was identified by the SEM investigation using Tescan Vega 3 LMH instrument (Czech Republic) (**Fig. 1**).

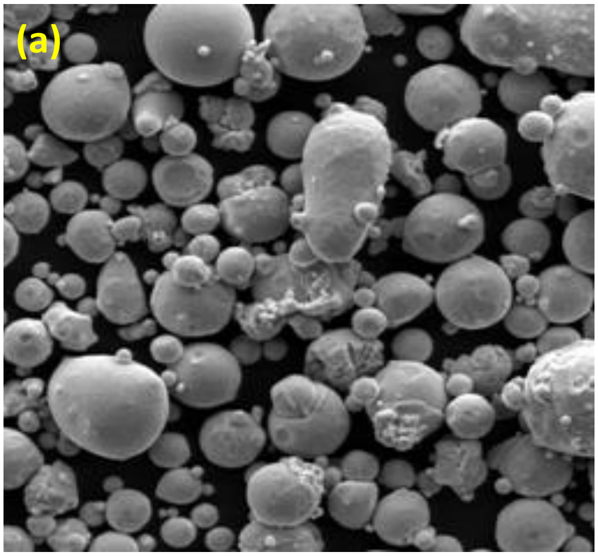

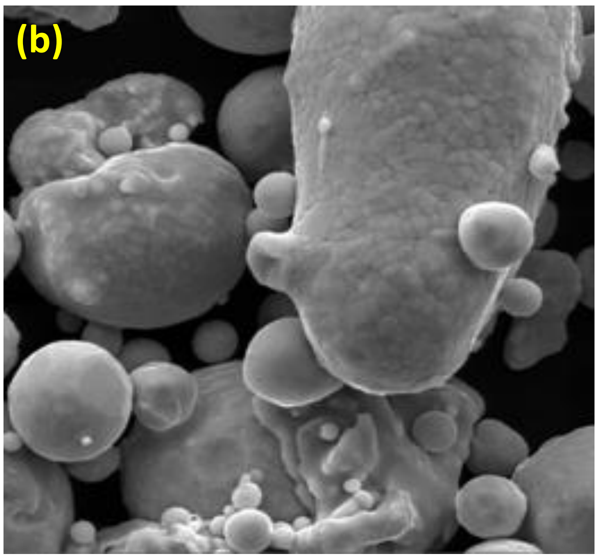

Fig. 1. SEM images of CoCrMo powder x1200 (a) and x4000 (b).

A granulometric analysis was made by Alpaga 500 nano instrument (Occhio SA, Belgium). The statistical distribution of the particles was by equivalent diameter of d5= 14.5 µm, d50= 30.3 µm, d95= 45.9 µm with a mean equivalent diameter about 30 µm. 67. One percent of particles have spherical morphology, meanwhile 2.4 percent of them have irregular morphology (**Fig. 2**).

Because of the limited space for experimental work and a significant quantity of the used optical equipment, the melting processes were produced without any additional protective cover or protective atmosphere. The previous practice of work with CoCrMo powder for SLM showed that this material has the largest heat resistance in comparison with other popular materials such as Ti_6Al_4V or maraging steel. The chemical composition is provided in **Table 1**. The powder layer thickness was measured by optical microscope Olympus BX51M (Japan). For the experiments, the powder was sieved, blended and dehumidified by means of heating at the temperature of 100 °C within four hours. The carbon steel C1020 was used as a substrate.

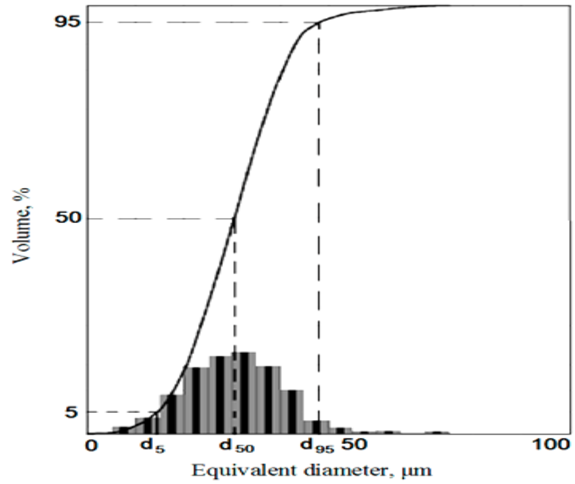

Fig. 2. Granulometric analysis of CoCrMo powder.

For the purpose of creating a smoother temperature gradient and the optimal conditions of the heat and mass transfer in the melting pool, an experimental stand for SLM-processing with the system of laser beam power density distribution modulation was created.

The experimental stand includes a laser source such as a continuous-wave Ytterbium fiber laser LK-200-V with the wavelength of λ=1.07 µm (IPG Photonics, Russia) and the maximum power P=200 W. The collimated laser beam has an effective diameter of 5 mm after optical collimator. The laser beam movement according to the programmed trajectory in the working area was produced by the scanning system. The pi-shaper module for the transformation of the Gaussian laser power distribution according to the principles of aspherical optical surfaces refraction was placed between the scanning head and the laser source. The laser beam goes through f-theta focusing lens which enlarge marked square for laser treatment. Afterwards, the beam is projected on the working surface for powder layer melting. The laser beam profile is controlled by the optical system that includes an optical mirror BCube, an attenuator and a CCD-camera LaserCam-HRTM. The signal register by a CCD-camera, but the technical characteristics of the asset do not allow processing of the laser source with power more than 4 W. It is the reason to pace an attenuator between the CCD-camera and BCube. The attenuator is a passive asset to weaken a signal in several times before sending it to the camera. The signal goes to PC. The customized software is installed on the PC to process the signal and to represent it to the operator on the display.

The optical monitoring system consists from a high-speed CCD-camera Photron SA5 (Japan). The CCD-camera records the visible range of SLM-processing. The maximum speed of the camera is 775000 FPS, the maximum resolution is 1024×1024 pixels. The laser backlight Cavilux is used for lighting a work area and for functional needs of the camera. The laser backlight is also equipped with a light filter which protects the obtained image from generated light, and with a macro objective

Navitar 6000 for tiny process details recording with higher magnification. The IR camera of down ranging is installed for extra data receipt about thermal influences of processing. The IR camera has the resolution of 560×760 pixels and release time of 3 msec. The calibration of this asset is produced by blackbody in the temperature range of 1200-1800 ^{o}C. The two-wave pyrometer is used for measuring the temperature in the laser beam treatment area for the temperature range of 1200-2900 K.

The mechanical part of the stand is described in [**1**]. The geometrical tolerance for the working surfaces was ± 0.02 mm. In the experiments, a layer of powder is deposited on the working surface. The thickness of each layer (80 µm (±5 µm)) was controlled by the optical microscope in three different points.

In accordance with the focus distance of F-theta lens of 420 mm, the working surface was placed at such distance to attain the maximum energy concentration on the powder surface. The placement of the working platform was fixed as initial placement of the working surface.

In accordance with the special features of the experimental stand and for reducing the error influence of the rotate ring on the optical tool such as piShaper, an optical system was fixed. Hence, the changes of the power distribution were produced by distance changes from the working surface to the focus lens. The effective diameter of the laser beam (86.5 %) was defined by the CCD-camera as 0.111 mm, the effective area was 0.261 mm^2.

For the calculation of the distance between different distributions, the next formula has been used:

$$R = \frac{8\lambda f'^2}{\pi D^2} \tag{1}$$

where, λ - laser wave length, f'- focus distance, F-theta lens, D - laser beam diameter after collimator.

The other distributions are placed on the distance 20 mm. For this purpose the working surface was moved. The flat-top and inverse Gaussian distributions (**Fig. 3** (**b**) and (**c**)) were achieved by this method. They were defined by the CCD-camera: The movements of the working surface (powder layer on the working platform) were produced for the experimentation work as described in [**1**]. The effective diameter and area are presented in **Table 2**.

Table 2. Effective diameter and area for donut and flat-top laser beam distributions.

Laser beam distribution	Effective diameter, mm	Effective area, mm^2
Donut distribution	0.347	0.124
Flat-top distribution	0.260	0.165

The metallographic samples of single tracks were prepared by conventional methods using the technological complex ATM (Germany). The single tracks was studied by the optical microscope Olympus BX51 (Japan) and by the scanning electronic microscope Tescan Vega 3 LMH (Czech Republic).

The high-velocity camera Photron SA5 was used for the monitoring of the processes in the molten pool. For excluding the influence of the laser beam light and thermal radiation the laser diode illumination with the 810 nm filter was used. There were selected next parameters of the recording: frame rate and pulse frequency of illumination 1000 Hz, 1024x1024 pixels resolution, shutter 999 microseconds.

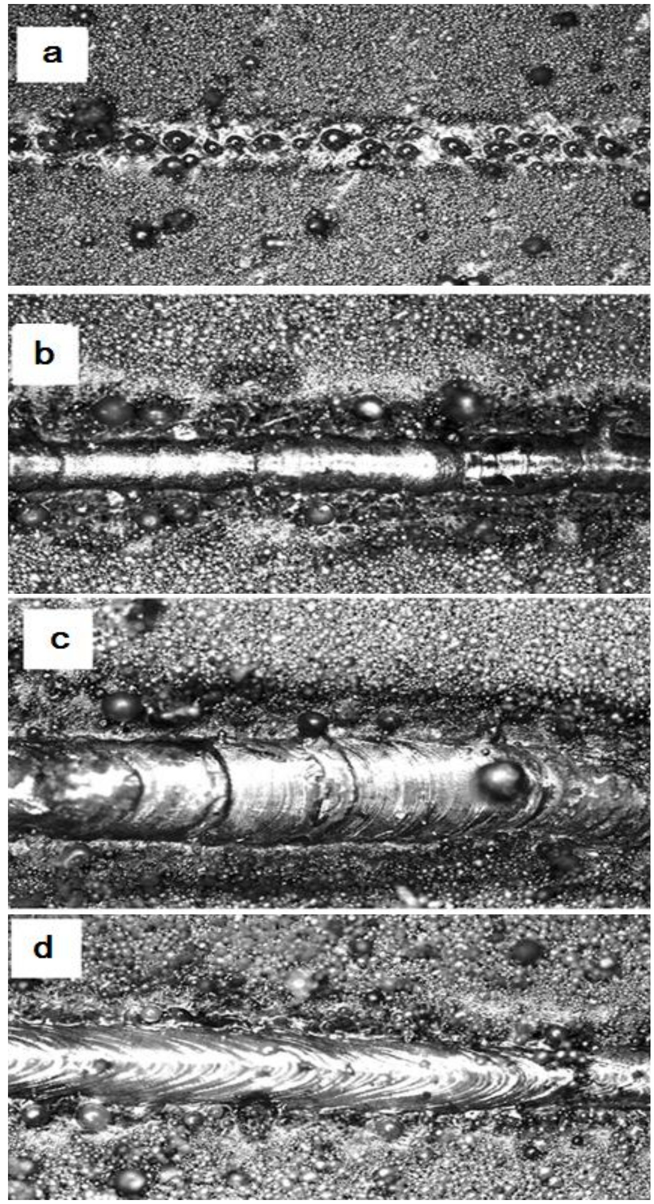

Fig. 3. SLM-tracks images obtained by optical microscope: P=10 W, Vs=30 mm/sec (a); P=70 W, Vs=10 mm/sec (b); P=170 W, Vs=5 mm/sec (c); P=200 W, Vs=60 mm/sec (d).

Results and discussion

The single tracks were produced by the obtained laser power density distribution. Two SLM-process parameters were varied for each obtained distribution: laser power in the range of P=10-200W and scanning speed of Vs=5-100 mm/sec. The two main technological gaps were discovered for SLM-processing of stable track formation (**Table 3**): for Gaussian P=30-70W, Vs =5-20 mm/sec and P=130-150 W, Vs=40-70 mm/sec; for Flat-top P=50-70W, Vs=5-20 mm/sec and P=130-200 W, Vs=40-80 mm/sec; for Inverse

Gaussian P=70-130W, Vs=5-20 mm/sec and P=150-200 W, Vs=40-100 mm/sec (**Table 3**).

Table 3. Results of experimental work for SLM-processing of single tracks.

Laser beam power (P), W	Scanning speed (V_S), mm/sec 5	10	20	30	40	50	60	70	80	100
Gaussian laser power density distribution										
10	0	0	0	0	0	0	0	0	0	0
30	+	+	+	-	-	-	0	0	0	0
50	+	+	+	-	-	-	-	-	-	-
70	+	+	+	+	-	-	-	-	-	-
100	++	++	-	+	-	-	-	-	-	-
130	++	++	++	-	-	+	+	+	-	-
150	++	++	+	+	+	+	+	+	+	-
170	++	++	+	-	-	+	+	+	+	+
200	++	++	++	++	+	++	-	+	-	+
Flat-top laser power density distribution										
10	0	++	0	0	0	0	0	0	0	0
30	+	-	-	0	0	0	0	0	0	0
50	-	+	-	-	-	-	-	-	-	-
70	+	+	+	-	-	-	-	-	-	0
100	++	++	-	-	-	-	+	+	+	+
130	++	++	++	+	+	+	-	+	+	0
150	++	++	++	+	-	+	+	-	-	-
170	++	++	+	+	+	+	+	+	+	0
200	++	++	++	++	++	+	+	+	-	+
Inverse Gaussian laser power density distribution										
10	0	0	0	0	0	0	0	0	0	0
30	0	0	0	0	0	0	0	0	0	0
50	-	-	-	-	-	0	0	0	0	0
70	+	+	-	-	-	-	-	-	-	-
100	+	+	+	-	+	-	-	-	-	-
130	++	+	+	+	-	-	-	-	0	-
150	++	++	++	-	+	-	+	+	+	-
170	++	++	++	+	++	+	+	+	+	+
200	++	++	-	++	+	+	+	-	+	+

0 full absence of metallurgical contact
+ stable track formation
++ too deep relative track depth
- non-stable metallurgical contact with subtract

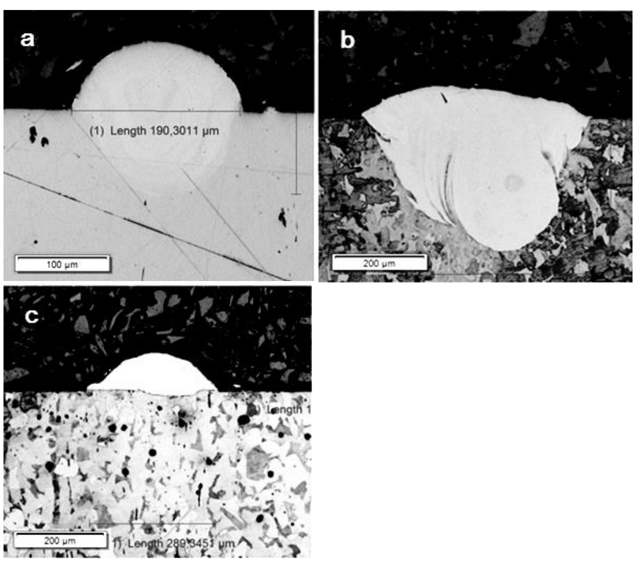

Fig. 4. SLM-track defects obtained on cross-sections by optical microscope: P=70 W, Vs=10 mm/sec (a); P=170 W, Vs=5 mm/sec (b); P=200 W, Vs=60 mm/sec (c).

For the defects of single tracks obtained by SLM-processing, see **Fig. 3** and **6**. The stable track formation was only produced in the technological gaps. The lower laser power gives full absence of the metallurgical contact between track and substrate (**Fig. 3**(**a**)) and lower scanning speed gives too deep relative track depth (**Fig. 3**(**a**), **Fig. 4**(**b**)). In the latter case, the laser melts the obtained track continuously with lower object layers resulting in non-homogeneous structure of the 3D-objects and significantly increased melting pool. The higher scanning speed gives non-stable metallurgical contact between track and substrate (**Fig. 3**(**d**); **Fig. 4**(**c**)).

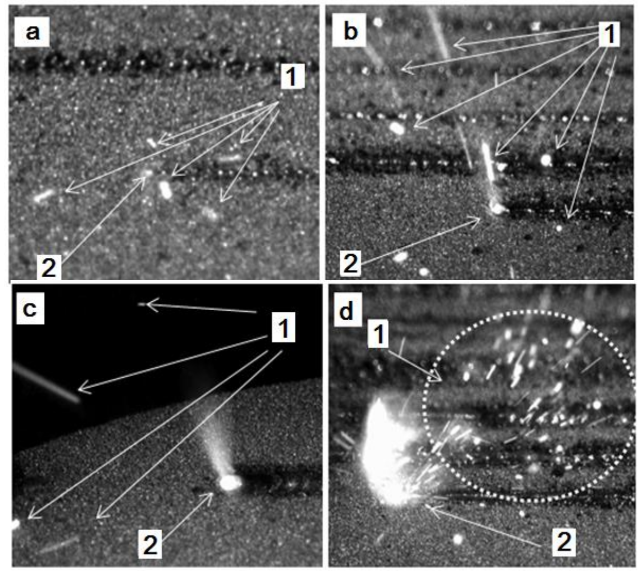

Fig. 5. Video monitoring of SLM-processing: P=10 W, Vs=30 mm/sec (a); P=70 W, Vs=10 mm/sec (b); P=170 W, Vs=5 mm/sec (c); P=200 W, Vs=60 mm/sec (d); 1 – powder granules; 2 – melt pool.

Video monitoring of the SLM-processing shows a higher material vaporization from the melting pool in the case of higher laser beam power and lower scanning speed. In **Fig. 5** (**c**) the lighting of vaporization is provided. The higher laser power and lower scanning speed give higher granule emission; see **Fig. 5** (**d**).

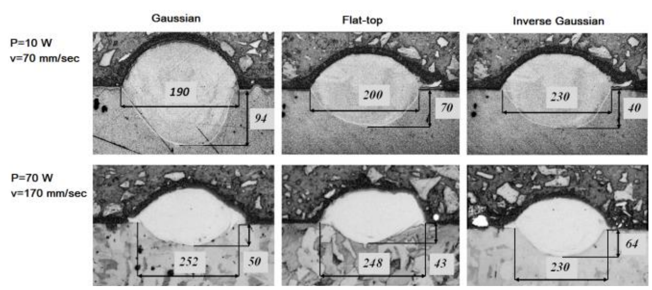

Fig. 6. Optical microscopy of single tracks, sizes in microns (µm).

Meanwhile, the technological gaps increase and move to the direction of power and scanning speed increase with the increase of laser beam effective diameter. Two groups of technological parameters were selected for two technological gaps: P=70W, Vs=10mm/sec and P=170W, Vs=70mm/sec (**Fig. 6**). These groups of the parameters are a good example of demonstrating the optical assets influence on the output parameters of single tracks. Meanwhile, the values P=200W and Vs=100 mm/sec are not the limits of technological gaps in the direction of parameters increase.

Conclusion

The study showed that the single SLM-tracks obtained by different laser power density distribution differ in their geometrical parameters and microstructure. The Flat-top distribution provides better metallurgical contact and considerably improves the quality of track melting into the substrate, where more homogeneous structure is observed by microscopy. These effects show promising results that laser power density distribution influences SLM-processing especially with laser power and scanning speed values increase. The results encourage to further studies of technological gap limits with higher values of input parameters and allow you to obtain SLM-processing with extra high productivity.

Acknowledgements
This work was financed by the Ministry of Education and Science of the Russian Federation within the frame of the state task in the field of scientific activity (№9.811.2014/K).

Author Contributions
Conceived the plan: AA, MV, AV; Performed the expeirments: IZh, SVF; Data analysis: PP, PP; Wrote the paper: AA, PP, PP. Authors have no competing financial interests.

Reference

1. Yadroitsev I.; Gusarov A.; Yadroitsava I.; Smurov I., *J. Mater. Proc. Tech.* **2010**, *210*, 1624.
   DOI: 10.1016/j.jmatprotec.2010.05.010
2. Gusarov A.V.; Yadroitsev I.; Bertrand Ph.; Smurov I., *App. Surf. Sci.* **2007**, *254 (4)*, 975.
   DOI: 10.1016/j.apsusc.2007.08.074
3. Okunkova A.; Volosova M.; Peretyagin P.; Vladimirov Yu.; Zhirnov I.; Gusarov A.V., *Ph. Proc.* **2014,** *56*, 48.
   DOI: 10.1016/j.phpro.2014.08.095
4. Okunkova A.; Peretyagin P.; Vladimirov Yu.; Volosova M.; Torrecillas R.; Fedorov S.V., *Proc. SPIE*, **2014**, *9135*.
   DOI: 10.1117/12.2053602
5. Hendriks A.; Naidoo D.; Roux F.S.; López-Mariscal C.; Forbes A., *Proc. SPIE*, **2012**, *8490*.
   DOI: 10.1117/12.932224

